



ELSEVIER

Separation and Purification Technology 00 (2002) 1–9

**Separation
and Purification
Technology**

www.elsevier.com/locate/seppur

5 Effect of electrostatic repulsive force on the permeate flux and
6 flux modeling in the microfiltration of negatively charged
7 microspheres

8 Sung-Wook Choi^a, Jung-Min Park^a, Yongsu Chang^a, Jeong-Yeol Yoon^b,
9 Seungjoo Haam^c, Jung-Hyun Kim^a, Woo-Sik Kim^{a,*}

10 ^a Nanosphere Process and Technology Laboratory, Department of Chemical Engineering, Yonsei University, 134 Shinchon-dong,
11 Sudaemoon-ku, Seoul 120-749, South Korea

12 ^b Department of Chemistry and Biochemistry, Biomedical Engineering IDP, University of California, Los Angeles, CA 90095, USA

13 ^c Fluid Mixing Technology Laboratory, Department of Chemical Engineering, Yonsei University, 134 Shinchon-dong, Sudaemoon-ku,
14 Seoul 120-749, South Korea

15 Received 21 February 2002; received in revised form 21 June 2002; accepted 21 June 2002

16 **Abstract**

17
18 A study on the permeate flux was performed in a stirred cell filled with monodispersed carboxylated microspheres
19 (polystyrene/polymethacrylic acid, PS/PMAA), to investigate the effects of surface charge (the number density of
20 surface carboxyl group, N_c ; 0.45, 5.94, 9.14, and 10.25 nm⁻²) and the stirrer speed (300, 400, and 600 rpm) under
21 constant transmembrane pressure. The permeate flux was found to be dependent on the surface charge, the ionic
22 strength, and the stirrer speed. The permeate flux was proportional to the surface charge of microspheres and inversely
23 proportional to the ionic strength because of electrostatic repulsive interaction and steric hindrance. The cake porosity
24 was estimated by Kozeny–Carman equation from the steady-state permeate flux data. Experimental data elucidated
25 that the cake porosity was extended from 0.211 to 3.04 upon the introduction of carboxyl group on the microsphere
26 surface, leading to the high permeate flux. Consequently, resistance-in-series model was employed for the modeling of
27 the permeate flux and showed a good agreement with the experimental results. © 2002 Published by Elsevier Science
28 B.V.

29 **Keywords:** PS/PMAA microspheres; Permeate flux; The number density of surface carboxyl group; Electrostatic interaction;
30 Resistance-in-series model

Nomenclature

A area (m²)
 d diameter (m)

3 * Corresponding author. Tel.: +82-2-2123-2753; fax: +82-2-312-0305

4 E-mail address: choisw94@empal.com (W.-S. Kim).

1 1383-5866/02/\$ - see front matter © 2002 Published by Elsevier Science B.V.

2 PII: S 1383-5866(02)00121-1

$J(t)$	permeate flux (m s^{-1})
k	rate of cake formation (s^{-1})
m	total dried mass of a cake layer (kg)
N	the number density of surface carboxyl group (nm^{-2})
R	resistance (m^{-1})
t	filtration time (s)
V	total volume of permeate
ΔP	transmembrane pressure (Pa)
z	distance (m)

Greek letters

ε	cake porosity (dimensionless)
κ	Debye–Hückel parameter (m^{-1})
μ	dynamic viscosity ($\text{Pa}\cdot\text{s}$)
ρ	density (kg m^{-3})
ψ	surface potential (mV)

Subscripts

c	cake layer (in R_c) or carboxyl group (in N_c)
m	Membrane
p	particle (in d_p) or permeate (in V_p)

Superscript

*	in steady-state
---	-----------------

31 1. Introduction

32 Membrane filtration has a great potential for
 33 removing colloidal suspensions such as clay parti-
 34 cles, proteins, and other macromolecules. How-
 35 ever, the major obstacle in membrane filtration is
 36 the flux decline due to the concentration polariza-
 37 tion and the fouling. During filtration of colloidal
 38 suspensions, particles are driven onto the mem-
 39 brane surface where they accumulate and form a
 40 cake or gel layer. This particle build-up is known
 41 as a concentration polarization, and results in
 42 increasing of the hydraulic resistance to permeate
 43 flux.

44 Many researchers have studied on the variation
 45 and modeling on the flux decline. Bhattacharjee [1]
 46 had developed the predictive model for the flux
 47 decline in unstirred and stirred batch cells by
 48 unifying the osmotic pressure and gel layer model.

These analyses were mostly suitable for the filtra- 49
 tion of an aqueous solution of low molecular 50
 weight solutes (osmotic pressure controlled) and 51
 high molecular weight solutes (gel layer con- 52
 trolled). A force balance model was also developed 53
 to predict the effects of particle size, particle size 54
 distribution, and surface potential on the structure 55
 of the cake layer [2]. Crossflow filtration of 56
 monodispersed polystyrene latex ranging from 57
 0.064 to 2.16 μm in diameter was studied under 58
 constant transmembrane pressure mode by Lee 59
 and Clark [3]. Besides the crossflow filtration tests, 60
 dead-end filtration test were also carried out to 61
 independently determine a model parameter, the 62
 specific cake resistance. Benkahla et al. [4] studied 63
 on the fouling mechanism in filtration of a mineral 64
 CaCO_3 suspension using Ergun's equation and 65
 Darcy's law. Hamachi [5] has used a conventional 66
 crossflow microfiltration pilot with a laser device 67

68 to measure deposit thickness and studied on the
69 effect of accumulative volume, time, and trans-
70 membrane pressure on the thickness of deposition.

71 There were several studies [2,6,7] about the
72 influence of surface interaction on permeate flux.
73 McDonogh et al. [6] conducted cross-flow ultra-
74 filtration experiments using non-flocculating silica
75 particles. They studied the charge effect of the
76 particles and the retentate permeability on mem-
77 brane performance. Bacchin [7] reported that the
78 critical flux of clay suspensions decreased to zero
79 by adhesion as increasing the salt concentration.
80 The reduction of surface repulsive force was
81 responsible for such changes. These researches
82 generally adjusted the repulsive force of particle
83 by controlling ionic strength, pH, and salt con-
84 centration. In this paper, however, the charge
85 effect of microsphere itself was mainly investigated
86 on the permeate flux. The surface charges of
87 microspheres with same particle size were varied
88 by co-polymerization of styrene and methacrylic
89 acid.

90 This paper is focused on the effect of surface
91 charge of polystyrene/polymethacrylic acid micro-
92 spheres (PS/PMAA) on the flux behavior and the
93 modeling of permeate flux by resistance-in-series
94 equation. These results were used for the basic
95 data for the protein separation systems previously
96 proposed in our group [8]. In the first section, the
97 surface charge effect of microspheres on the flux
98 behavior was studied in various conditions (the
99 number density of surface carboxyl group, stirrer
100 speed, ionic strength). In the second part, these
101 experimental results were fitted to the theoretical
102 model. From these analyses, the cake porosity and
103 the flux behavior were studied in detail.

104 2. Experiment

105 2.1. Materials

106 Styrene (St) and methacrylic acid (MAA) were
107 from Junsei Chemical Co. (Japan) and used as
108 monomers for the copolymerization after a pur-
109 ification with Aldrich's inhibitor remover column
110 (catalog number 306312). Potassium persulfate
111 (KPS, Samchun Pure Chemical Ind., Ltd., Korea)

112 was used as an initiator for co-polymerization.
113 Synthesized microspheres were purified by mixed-
114 bed ion exchange resins (Dowex MR-3, Sigma
115 Chemical Co., USA, catalog number I-9005). An
116 acetic buffer of pH 4.5 was made of sodium acetate
117 and acetic acid (both from Yakuri Pure Chemicals
118 Co., Ltd., Japan). A polyether sulfone (PES)
119 planar membrane (Orange Scientific Co., Belgium)
120 with pore size of 0.2 μm was used for the
121 microfiltration study. All water used in the experi-
122 ments was distilled and deionized, produced by
123 Elgastat's UHQ system (UK).

124 2.2. Preparation and characterization of 125 microspheres

126 St and MAA were used as a main monomer and
127 co-monomer, respectively, where the surface car-
128 boxyl group will be given by hydrophilic MAA.
129 Soap-free emulsion polymerization was performed
130 in a 1.5 l internally stirred jacketed reactor at
131 70 °C, and nitrogen gas was purged in small doses
132 to provide nitrogen atmosphere. Low carboxy-
133 lated microsphere (CM-1) was prepared by batch
134 copolymerization and highly carboxylated ones
135 (CM-2, 3, and 4) were prepared by the two stage
136 shot growth method [9]. Tables 1 and 2 give the
137 recipes for the synthesis of PS/PMAA micro-
138 spheres with various number density of surface
139 carboxyl group.

140 The microspheres were purified by mixed-bed
141 ion-exchange resins and further purified by serum
142 replacement method [10]. The serum replacement
143 procedure was performed in a 400 ml stirred cell
144 (Amicon, Model 8400, USA) equipped with 0.2
145 μm membrane filters. The particle diameter of
146 microspheres was assessed by Scanning Electron
147 Microscopy (JEOL, Japan) and the number den-
148 sity of surface carboxyl groups was determined

Table 1
Recipe for the low carboxylated PS/PMAA microspheres
(batch copolymerization)

	St (g)	MAA (g)	KPS (g)	D.D.I. water (g)
CM-1	60	0.6	0.24	600

Table 2

Recipe for the highly carboxylated PS/PMAA microspheres (two stage shot growth method) [9]

First stage		Second stage (injected at conversion 90%)		
St (g)	60	CM-2	MAA	1.5 (g)
MAA (g)	0.6	CM-3	MAA	3.0 (g)
KPS (g)	0.24	CM-4	MAA	6.0 (g)
D.D.I Water (g)	600			

149 using conductivity meter (HI 8633 conductivity
150 meter, Portugal) using NaOH solution as a titrant.

151 2.3. Procedure of microfiltration

152 The experimental set-up is schematically shown
153 in Fig. 1. A stirred cell (50 ml, Amicon, model
154 8050, USA) with a 0.2 μm membrane filter
155 (Orange Scientific Co., Belgium) was filled with
156 30 ml dispersion of microspheres (0.47 g micro-
157 spheres per 30 ml). The specific surface area was
158 0.19 m^2 per 1 ml and the ionic strength was 0.01,
159 which were the same conditions of our previous
160 studies [11]. At a constant stirrer speed, acetic

161 buffer (pH 4.5) was introduced into the stirred cell
162 until the permeate flux was in steady state. The
163 permeate flux was continuously measured with an
164 electronic balance (precision plus, Ohaus Co.,
165 USA). The electronic balance was connected to a
166 PC through a RS 232 C interface. The number
167 density of surface carboxyl group (N_c) of micro-
168 spheres was varied as 0.45, 5.94, 9.14 and 10.25
169 nm^{-2} , and the stirrer speed was varied as 300, 400
170 and 600 rpm. The filtration of pure water without
171 microsphere was performed to determine mem-
172 brane resistance (R_m). All experiments were con-
173 ducted in three times.

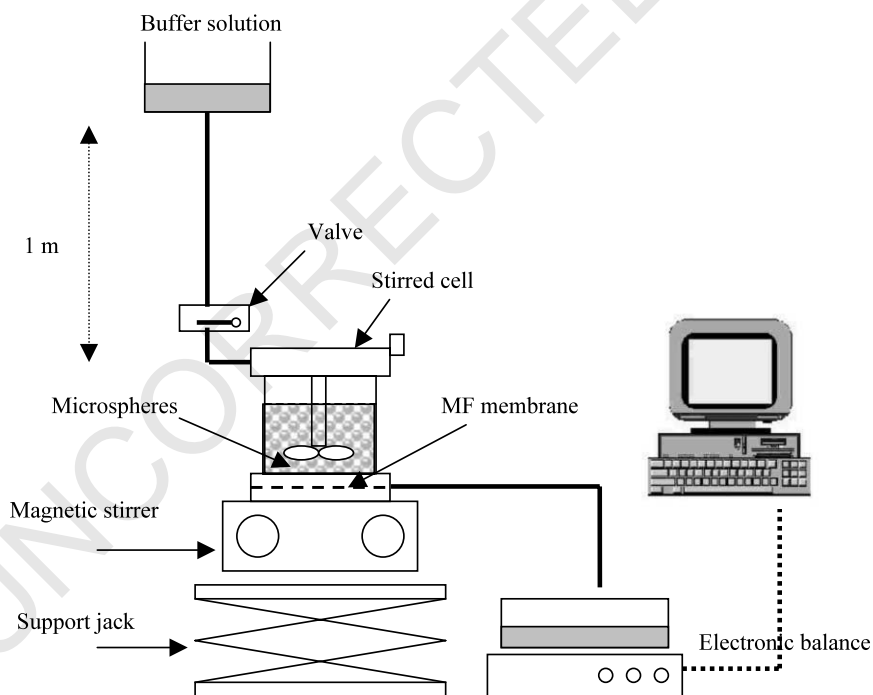


Fig. 1. Experimental apparatus for microfiltration.

Table 3
Characterization results of the various monodisperse microspheres

	CM-1	CM-2	CM-3	CM-4
d_p (nm)	478	481	480	485
N_c (nm ⁻²)	0.45	5.94	9.14	10.25

174 3. Results and discussion

175 The particle size and the number density of
176 surface carboxyl group of various microspheres
177 are shown in Table 3. All microspheres have a
178 polydispersity index near unity (1.009 determined
179 by Capillary hydrodynamic Fractionation, CHDF-
180 1100, Matec Applied Sciences, USA) and the same
181 particle size to investigate the effect of surface
182 charge only.

183 3.1. Study on the steady-state permeate flux

184 The permeate flux initially decreased with time
185 due to the formation of a cake layer during
186 microfiltration and then reached steady state.
187 Fig. 2 shows the steady-state permeate flux with
188 respect to the number density of surface carboxyl

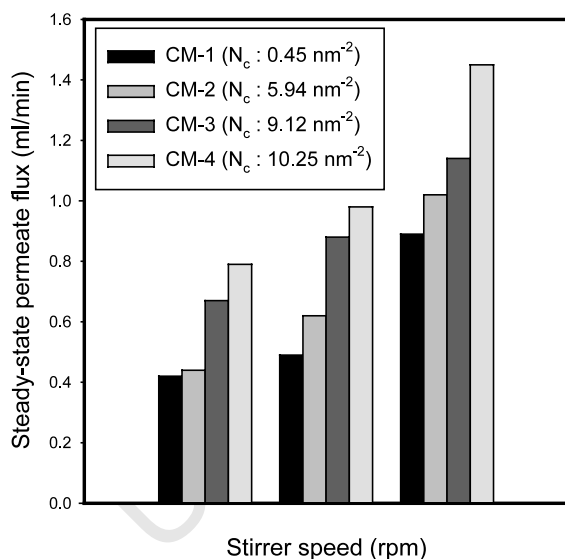


Fig. 2. Steady-state permeate flux with different stirrer speeds and the number densities of surface carboxyl group.

189 group and stirrer speed. The faster the stirrer
190 speed, the higher the permeate flux because of the
191 high shear stress at the surface of a cake layer. The
192 permeate flux was found to be increased with N_c ,
193 because the high repulsive force resulted in the
194 increase of effective radii of microspheres. There-
195 fore, the larger cake porosity and steric hindrance
196 could be achieved, leading to the large permeate
197 flux. The change of the cake porosity was calcu-
198 lated by resistance-in-series model (results shown
199 in Section 3.2). Fig. 3 gives the schematic explana-
200 tion of the effect of surface charge on the permeate
201 flux.

202 Fig. 4 shows the permeate flux of CM-4 through
203 membrane at stirrer speed of 400 rpm with respect
204 to the ionic strength. The high ionic strength (0.1)
205 results in decreased thickness of electric double
206 layer. The electrical potential exponentially de-
207 creases over the distance from surface according to
208 the following Debye–Hückel approximation
209 [12,13];

$$\psi = \psi_0 \exp(-\kappa z) \quad (1) \quad 210$$

211 where ψ , surface potential at distance z (mV); ψ_0 ,
212 surface potential (mV); κ , the Debye–Hückel
213 parameter (m⁻¹) and z , distance (m).

214 The parameter κ is directly related to the
215 electrolyte concentration and identified as recipro-
216 cal of the thickness of the electrical double layer.
217 Upon decreasing the ionic strength, the thickness
218 of electrostatic double layer around the particle
219 surface increases, leading to the increased perme-
220 ate flux. It was reported that permeate flux in
221 crossflow filtration (or dead-end filtration) was
decreased at a higher ionic strength condition,

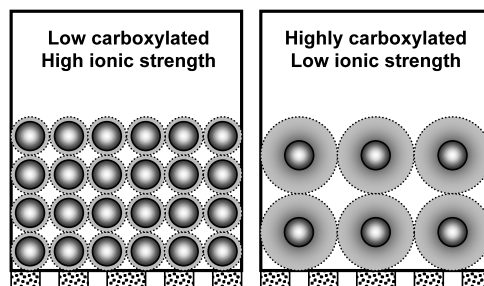


Fig. 3. Schematic diagram illustrating the effect of surface charge on permeate flux.

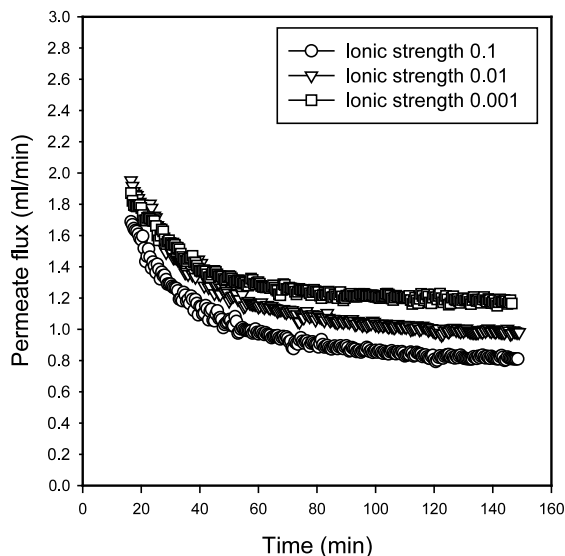


Fig. 4. Effect of ionic strength on the permeate flux with time in CM-4 ($N_c = 10.25 \text{ nm}^{-2}$, at 400 rpm).

because the decreased Debye screening length with increasing ionic strength resulted in a denser cake layer [14,15]. As a consequence, the increase of the ionic strength results in a compressed cake layer.

3.2. Cake porosity

The cake porosity was closely related to the surface charge of microspheres and can be estimated from the steady-state flux data using Kozeny–Carman equation and resistance-in-series model. There are two unknown variables such as the total mass of a cake layer (m_p) and the cake porosity (ϵ).

The total particle mass of a cake layer which mainly depends on the stirrer speed, can be determined as follows [11]; The permeate concentration of microsphere was nearly zero because the membrane pore size was small enough to retain all microsphere in our system. The concentrations were indirectly measured by UV spectrophotometer (UV-160A, Shimadzu, Japan). There was a linear relationship between concentration of microsphere and absorbance. When the permeate flux was in the steady state, the absorbance of retentate was measured. The absorbance of retentate was measured when the permeate flux has

reached the steady state. The total particle mass of a cake layer was inversely proportional to the stirrer speed, because increased stirrer speed caused the thickness of a cake layer to decrease. Lee and Clark [3] demonstrated that the specific cake resistance ($= 180(1-\epsilon)/d_p^2\epsilon^3$) remained fairly constant during dead-end filtration in the condition of complete rejection, which implying constant cake porosity as assumed.

The cake porosity obtained from the steady-state flux, is plotted against N_c in Fig. 5. The cake porosity was observed to be increased with N_c . The increase of effective radii of microspheres was responsible for the large cake porosity. Similar interpretation was used in the other researches [6,16]. Chang et al. [16] reported that the permeate flux decreased with the increase of the electrolyte concentration of the suspension. This can be explained by assuming both the interparticle distance and repulsive force to be decreased with the higher electrolyte concentration.

When the particle size of uncharged polystyrene microsphere was 480 nm, the cake porosity was 0.211, which was calculated from the empirical equation reported by the Lee and Clark [3]. However, it can be extended by an introduction of carboxyl group on the microsphere surface. If

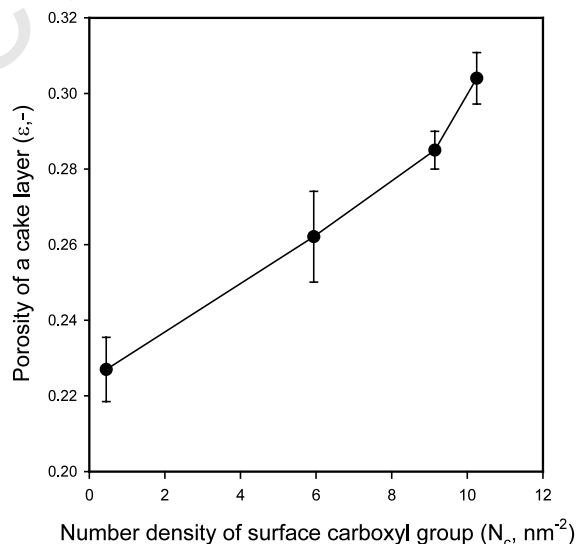


Fig. 5. Calculated cake porosity with the number density of surface carboxyl group.

the surface of microsphere is fully modified with methacrylic acid (in the case of CM-4), the cake porosity is 0.304. The cake porosity was significantly dependent on the thickness of electric double layer (or the effective radius of the particle), which could be varied by the number density of surface carboxyl group and ionic strength.

3.3. Modeling of the permeate flux

Two parameters are required for modeling of the permeate flux; the cake porosity (ε) and the total dried mass of a cake layer (m_p) (determined in Section 3.2.), assumed to be dominantly affected by surface charge of microspheres and stirrer speed, respectively. Resistance-in-series model was employed for the modeling of the permeate flux. In our system, the permeate concentration of microsphere was nearly zero because the membrane pore (200 nm) size was small enough to retain all microspheres (480 nm). Therefore, total resistance is the sum of the membrane and cake resistance. The permeate flux (J) can be expressed as follows,

$$J(t) = \frac{1}{A_m} \frac{dV_p}{dt} = \frac{\Delta P}{\mu(R_m + R_c)} \quad (2)$$

where $J(t)$, permeate flux (m s^{-1}); V_p , total volume of permeate; A_m , membrane area (m^2); ΔP , transmembrane pressure (Pa); μ , dynamic viscosity ($\text{Pa}\cdot\text{s}$); R_m , membrane resistance (m^{-1}) and R_c , cake resistance (m^{-1}). R_m can be evaluated from the flux measurement of pure water. From Kozeny–Carman equation, cake resistance can be written as follows

$$R_c = 180 \frac{(1 - \varepsilon)^2}{d_p^2 \varepsilon^3} \frac{m_p}{(1 - \varepsilon) A_m \rho_p} = \frac{180(1 - \varepsilon)m_p}{d_p^2 \varepsilon^3 A_m \rho_p} \quad (3)$$

where m_p , total dried mass of a cake layer (kg); d_p , particle diameter (m); ρ_p , density of particle (kg m^{-3}) and ε , cake porosity (–).

For the modeling of permeate flux, total dried mass of a cake layer should be defined as the

function of time and may be written as following equation.

$$m_p(t) = m_p^*(1 - \exp(-kt)) \quad (4)$$

m_p^* is the total dried mass of a cake layer in the steady-state permeate flux and k is the rate of cake formation. Similar equation was used by Gekas et al. [17]. Therefore, cake resistance can be expressed as follows,

$$R_c = \frac{180(1 - \varepsilon)m_p^*(1 - \exp(-kt))}{d_p^2 \varepsilon^3 A_m \rho_p} \quad (5)$$

The cake porosity was determined from the flux data in steady-state, and this is a key factor to the permeate flux. The cake porosity can be assumed to be constant during filtration [3] and the total dried mass of a cake layer (m_p^*) was a function of stirrer speed and time. The k value can be obtained by a non-linear regression from experimental flux data. The other necessary parameters were as follows: dynamic viscosity (μ) = 0.001 Pa·s, membrane area (A_m) = 0.00134 m^2 , particle density (ρ_p) = 1.05 kg m^{-3} , and membrane resistance (R_m) = 1.62 $\times 10^8 \text{ m}^{-1}$. The experimental results were compared with the modeling results in Figs. 6–8. The modeling results of the permeate

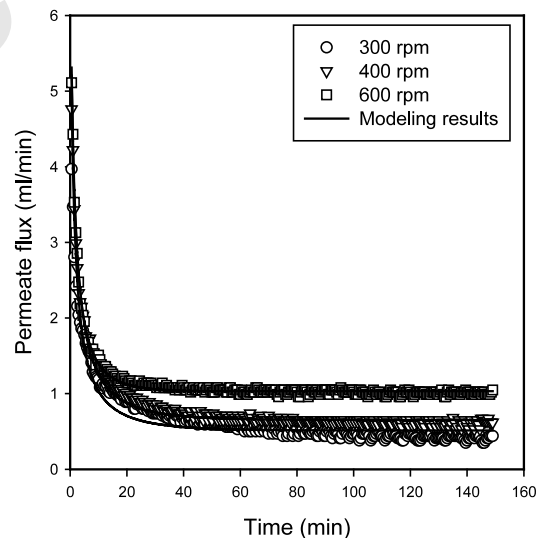


Fig. 6. Comparison of modeling results with experimental data in CM-2 ($N_c = 5.94 \text{ nm}^{-2}$).

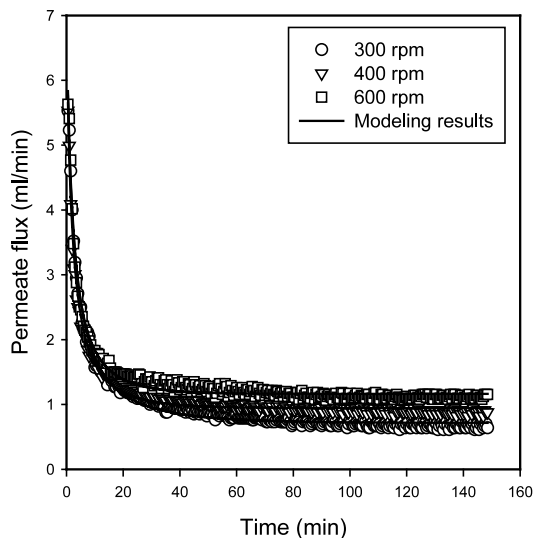


Fig. 7. Comparison of modeling results with experimental data in CM-3 ($N_c = 9.12 \text{ nm}^{-2}$).

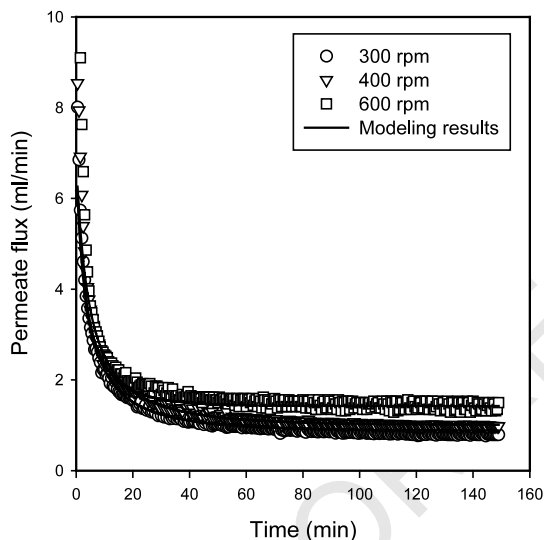


Fig. 8. Comparison of modeling results with experimental data in CM-4 ($N_c = 10.25 \text{ nm}^{-2}$).

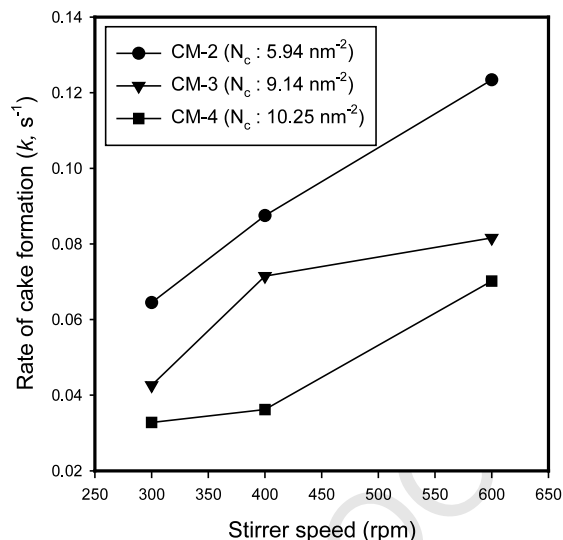


Fig. 9. The rate of cake formation at different stirrer speeds and the number densities of surface carboxyl group.

3.4. Behavior of the permeate flux

333

The exact evaluation of the rate of cake formation, k , is essential for the flux modeling because the cake formation depends on the particle deposition onto the membrane surface. Fig. 9 shows the rate of cake formation with different stirrer speeds and the number densities of surface carboxyl group. The rate of cake formation was inversely proportional to N_c under constant stirrer speed. The increased N_c leads to a higher permeate flux and a longer time to equilibrate. This means that the cake layer is slowly formed in the filtration of microspheres with high surface charge, due to the repulsive force between microspheres. This phenomenon was due to the interparticle repulsion. The rate of cake formation was found to be increased with the stirrer speed in the same N_c condition, because the microspheres were rapidly accumulated onto the surface of membrane when the permeate flux was high. Consequently, large k value was observed when the microspheres with low surface charge was filtrated in the condition of high stirrer speed.

334

335

336

337

338

339

340

341

342

343

344

345

346

347

348

349

350

351

352

353

354

355

331 flux were in a good agreement with the experi-
332 mental data.

356 **4. Conclusion**

357 The effect of surface charge on the permeate flux
 358 was studied in the microfiltration using stirred cell
 359 filled with PS/PMAA microspheres. To obtain
 360 large permeate flux, the high surface charge, low
 361 ionic strength, and the high stirrer speed were
 362 required. The large cake porosity, which was
 363 induced by the increase of N_c and the decrease of
 364 ionic strength, was responsible for the large
 365 permeate flux. The cake porosity could be esti-
 366 mated from the experimental data at the different
 367 number densities of surface carboxyl group. It was
 368 extended from 0.211 to 0.304 by introduction of
 369 methacrylic acid onto microsphere surface. Resis-
 370 tance-in-series model was employed for the mod-
 371 eling of the flux variation. This model provides a
 372 useful tool to understand the effect of the electro-
 373 static repulsive force on the permeate flux.

374 **Acknowledgements**

375 The authors acknowledge the financial support
 376 of Bioproducts Research Center (1994S0018),
 377 Yonsei University and the Korea Institute of
 378 S&T Evaluation and Planning (National Research
 379 Laboratory Program, M1-9911-00-0044).

380 **References**

- 381 [1] S. Bhattacharjee, A. Sharma, P.K. Bhattacharya, A unified
 382 model for flux prediction during batch cell ultrafiltration,
 383 *J. Membr. Sci.* 111 (1996) 243.
 384 [2] L.F. Fu, B.A. Dempsey, Modeling the effect of particle
 385 size and charge on the structure of the filter cake in
 386 ultrafiltration, *J. Membr. Sci.* 149 (1998) 221.
 387 [3] Y. Lee, M.M. Clark, Modeling of flux decline during
 388 crossflow ultrafiltration of colloidal suspension, *J. Membr.*
 389 *Sci.* 149 (1998) 181.

- [4] Y.K. Benkahla, A. Ould-Dris, M.Y. Jaffrin, D. Si-Hassen, 390
 Cake growth mechanism in cross-flow microfiltration of 391
 mineral suspension, *J. Membr. Sci.* 98 (1995) 107. 392
 [5] M. Hamachi, M. Mietton-Peuchot, Experimental investi- 393
 gation of cake characteristics in crossflow microfiltration, 394
Chem. Eng. Sci. 54 (1999) 4023. 395
 [6] R.M. McDonogh, C.J.D. Fell, A.G. Fane, Surface charge 396
 and permeability in the ultrafiltration of non-flocculating 397
 colloids, *J. Membr. Sci.* 21 (1984) 285. 398
 [7] P. Bacchin, P. Aimar, V. Sanchez, Influence of surface 399
 interaction on transfer during colloid ultrafiltration, *J.* 400
Membr. Sci. 115 (1996) 49. 401
 [8] J.Y. Yoon, J.H. Lee, J.H. Kim, W.S. Kim, Separation of 402
 serum proteins with uncoupled microsphere particles in a 403
 stirred cell, *Colloid. Surf. B* 10 (1998) 365. 404
 [9] J.H. Kim, M. Chainey, M.S. El-Aasser, J.W. Vanderhoff, 405
J. Polym. Sci. A 27 (1989) 3187. 406
 [10] M.S. El-Aasser, in: M.S. El-Aasser (Ed.), *Advances in* 407
Emulsion Polymerization and Latex Technology, vol. 2 408
 (Lecture 3), Emulsion Polymers Institute (Lehigh Univer- 409
 sity), Bethlehem, PA, 1984. 410
 [11] S.W. Choi, J.Y. Yoon, S. Haam, J.K. Jung, J.H. Kim, 411
 W.S. Kim, Modeling of the permeate flux during micro- 412
 filtration of BSA-adsorbed microspheres in a stirred cell, *J.* 413
Colloids Interf. Sci. 228 (2000) 270. 414
 [12] D. Myers, *Surfaces, Interfaces, and Colloids: Principles* 415
and Applications, VCH Publishers, New York, 1991, p. 416
 76. 417
 [13] R. Buscall, T. Corner, J.F. Stageman, *Polymer Colloids*, 418
 Elsevier Applied Science Publishers, New York, NY, 1985, 419
 p. 144. 420
 [14] R.S. Faibish, M. Elimelech, Y. Cohen, Effect of inter- 421
 particle interaction on flux decline in crossflow membrane 422
 filtration of colloidal suspensions, *Proceedings, Ninth* 423
Annual Meeting, North American Membrane Society, 424
 Baltimore, 1997. 425
 [15] M.S. Chun, G.Y. Chung, J.J. Kim, On the behavior of the 426
 electrostatic colloidal interaction in the membrane filtra- 427
 tion of latex suspensions, *J. Membr. Sci.* 193 (2001) 97. 428
 [16] D.J. Chang, F.C. Hsu, S.J. Hwang, Steady state permeate 429
 flux of cross-flow microfiltration, *J. Membr. Sci.* 98 (1995) 430
 97. 431
 [17] V. Gekas, P. Aimar, J.P. Lafaille, V. Sanchez, A simula- 432
 tion study of the adsorption–concentration polarization 433
 interplay in protein ultrafiltration, *Chem. Eng. Sci.* 48 434
 (1993) 2753. 435